177. Numerical Simulation of an active phased-array spaced-antenna weather radar

V. Venkatesh, K. Orzel, S.J Frasier

Microwave Remote Sensing Laboratory, University of Massachusetts, Amherst, MA 01003, USA

ABSTRACT

In Engineering, complete control of the simulation environment is used to efficiently arrive at designs for subsequent implmentation and minimize trial and error. Here, a monte-carlo based phased-array weather radar simulator is developed. The results obtained are validated with theoretical predictions for the auto- and cross-spectra and the correlation function expectation. Future work includes using this simulator as a tool to better interpret observations made using the spaced-antenna system.

1. Introduction

The application of the spaced-antenna method, if proven practical for weather radars, is a potential means of single radar based high angular resolution wind-vector retrieval (Zhang and Doviak (2007), Pazmany et al. (2004)). However, to arrive at designs for spaced-antenna implementation and accurately interpret observations using a spaced-antenna weather radar, numerical simulations are essential.

Commonly used simulation techniques to mimic volume scattering scenarios seen by a radar include - methods that, having assumed a functional form for the spectra dither it, and immerse it in white noise (Zrnic (1975)) and methods that directly simulate backscattered E-fields at the antenna system (Holdsworth and Reid (1995), Cheong and Palmer (2008)). The former class of techniques assumes an apriori spectral shape and does not allow for modelling of physical processes. Since conditions that violate assuming the desired spectral shape might go unrecognized with this former class of methods, it has limited ability to engineer radar systems on. Here, we develop a phased-array weather radar simulator based on simulations of scatterer advection by spatially homogeneous mean wind and velocity turbulence. The following section presents our approach to SA aperture synthesis using an active phased-array antenna system and the simulation methodology to mimic the same. The obtained results are then validated with theoretical predictions.

2. Methodology

a. Considerations for spaced-antenna wind-estimation

Spaced-Antenna concepts have been reviewed in several works (Briggs et al. 1950; Briggs 1984; Larsen and Röttger 1989; Doviak et al. 1996; Holloway et al. 1997; Zhang and Doviak 2007), and can be explained through the cross-correlation function of back-scattered electric fields sampled by two mono-static antenna systems A_1 and A_2 separated by a baseline Δx. Effectively, spaced-antenna wind-estimation is based on a model for the correlation function expectation (or equivalently spectra) given by

$$\begin{aligned} |\gamma(\Delta x,\tau)| = \quad & \exp\{-k^2\phi_e^2[v_x\tau-\Delta x]^2\} \\ & \exp\{-k^2\theta_e^2 v_y^2\tau^2\} \\ & \exp\{-2k^2\sigma_{tz}^2\tau^2\} \end{aligned} \tag{1}$$

where, k is the radar wavenumber, Δx is the spaced-antenna baseline, σ_{tz} is the RMS radial velocity due to velocity turbulence, v_x and v_y are the respective along- and cross-baseline components of velocity, and ϕ_e and θ_e are standard deviations that describe the two way azimuth and elevation beamwidths respectively. These are related to conventional 3-dB beamwidths by $\phi_e = \frac{\phi'}{\sqrt{8ln2}}$ where ϕ' is the one way 3-dB beamwidth. The expression in (1) is the product of three Gaussian terms. The first describes the effect of the along-baseline wind on the correlation and is the term of primary interest. The second term describes the effect of cross-baseline winds. Small cross-baseline beamwidths reduce its impact. Together, these first two terms describe decorrelation due to a mean wind traversing a finite beamwidth antenna pattern and are denoted beam-broadening decorrelation. The third term in (1) describes the effect of velocity turbulence on the correlation. Being centered at zero-lag, the third term shifts the cross-correlation function towards zero-lag and reduces its absolute value. To mitigate the effect of velocity turbulence, the two antenna apertures must physically overlap to allow for SA wind estimation at microwave frequencies (Holloway et al. (1997)).

The University of Massachusetts is developing an X-band planar active phased-array antenna system that is

capable of electronic scanning in azimuth and mechanical actuation in elevation (Salazar et al. 2008). It consists of 64 element array of fan beam antenna elements. Behind each fan beam antenna element, transmit-receive modules provide ‘ programmable amplitude weighting on transmit and receive. Fig. 2 depicts our approach to implementing overlapped spaced apertures using this phased-array antenna system. The entire array aperture is used upon transmission, while alternating portions of the array are used upon reception. Auto and cross-correlations may be produced with the interleaved time series from separate portions of the array. The effective phase-centers of the overlapped apertures are located mid-way between the centers of the transmit and receive apertures. Therefore, with this implementation, the effective SA baseline is half the physical distance between the centers of the “left” and “right” receive apertures. This is similar to the scheme employed by the MAPR UHF radar (Cohn et al. 1997, 2001) and to that described using the NWRT S-band radar (Zhang and Doviak 2007). The primary strength of the phased-array is in the ability to synthesize various SA baselines and effective aperture sizes through the programmable amplitude-weighting on transmit and receive.

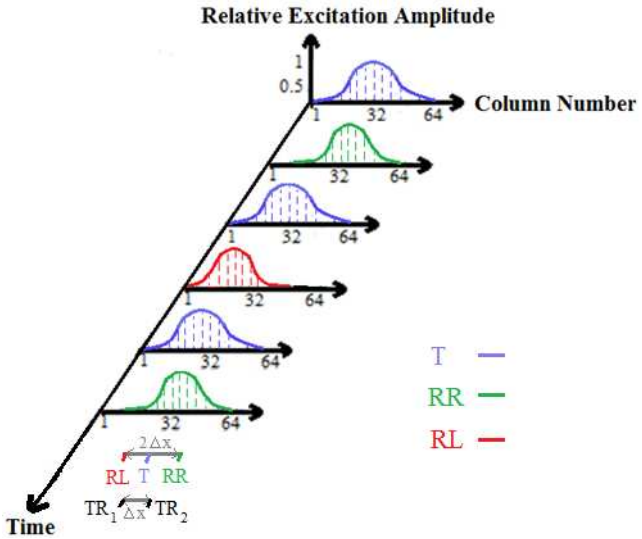

FIG. 1. Time series of transmit/receive aperture weighting indicating alternating left and right receive apertures interleaved with the transmit pulse.

b. Simulation of an active phased-array SA weather radar

Our approach to numerical simulations is to estimate correlation coefficients from simulated backscattered E-fields at spaced antennas using a weather radar simulator capable of generating two-dimensional (time and azimuth) data, similar to that described in Cheong and Palmer (2008) and Holdsworth and Reid (1995). The general structure of the simulation algorithm we use for our study is depicted in Fig. 2.

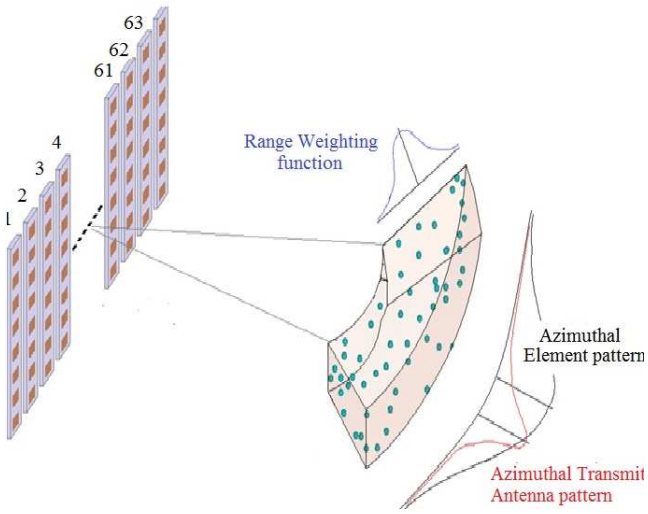

FIG. 2. Conceptual depiction of the phased-array weather radar signal simulator.

To initialize the simulator, the complex excitation coefficients of the phased-array antenna system, radar and meteorological parameters are prescribed. From these values, an enclosing volume centered on the illuminated footprint is defined. The dimensions of the initialized resolution volume are dictated by the smallest receive-aperture we wish to investigate for spaced-antenna aperture synthesis and the range resolution. This choice of the azimuthal dimension of the bounding-volume is, solely, to provide convenient run times for the simulation. Volume scattering is then simulated with random spatial sampling of (2)

$$V_J(t) = \Sigma_{n=1}^{n_s} A_{Jn} R_{Jn} exp\{-jk[r + r_{nJ}]\} \qquad (2)$$

where, $J = 1, 2, 3, ..., 64$ denotes the elements of the phased-array antenna system, A_{Jn} is the antenna weighting function and R_{Jn} is the range weighting function. The antenna weighting functions used to mimic a volume scattering scenario is given by (Doviak and Zrnić (1993), Zhang and Doviak (2007)).

$$A_{nJ}[r(t)] = exp\{-\frac{(X_0 - X(t))^2}{4r_0^2\phi_{T_e}^2} - \frac{(X_J - X_n(t)')^2}{4r_0^2\phi_{elem}}\} \; exp\{-\frac{(Y_0 - Y_n^1(t))^2}{2r_0^2\theta_e^2}\} \qquad (3)$$

where, $n = 1, 2, ..., n_s$ represents the scatterers within the resolution volume, ϕ_{T_e} is the azimuthal transmit beamwidth, ϕ_{elem} is the azimuthal element pattern beamwidth, θ_e is the effective 2-way elevational beamwidth. The range weighting function and its relationship to transmitted chirp bandwidth is given by (Doviak and Zrnić (1993))

$$R_n[r(t)] = exp\{-\frac{(Z_0 - Z_n(t)^{'})^2}{2\sigma_R^2}\} \quad (4)$$

$$\sigma_R = 0.35\frac{c}{2B} \quad (5)$$

where, c is the speed of light (m/s) and B is the transmitted chirp bandwidth. The constant 0.35 approximately accounts for losses due to amplitude modulation of the chirp and finite receiver bandwidth.

Scatterer locations are updated at every time-step corresponding to the pulse repitition interval based on the superposition of mean and turbulent velocity components along each co-ordinate. We use simple Gaussian distributed pseudo-random numbers to generate the turbulent velocity fields. Since the omission of temporal continuity of the velocity turbulence causes individual scatterers to have abrubt changes in the turbulent velocity (Holdsworth and Reid (1995)), we run a continuous 5-point moving average filter to low-pass filter the turbulent velocity spectrum in the temporal dimension (Cheong and Palmer (2008)). It is this low-pass filtering by the moving-average filter that distinguishes velocity turbulence from random Brownian motion or random changes in the phase of the composite signal introduced by thermal noise. Cheong and Palmer (2008) also report that abrubt changes in the spatial continuity of the velocity turbulence fields translate to errors in beam forming. We alleviate this problem by simply fixing the range to the radar resolution volume to be large.

Once the time- and azimuthal-series data are generated at each element, thermal noise is scaled and added directly to each element according to (6), assuming that the thermal noise generated at the elements are uncorrelated. Now, when the elements are combined, the signal power increases as N_R^2 , as the signal voltages add coherently. The noise power, however, only increases as N_R as they have random phase.

$$SNR_{elem} = \frac{SNR_{Rec-Array}}{64} \quad (6)$$

Finally, the time-series data are summed across several antenna elements and used to provide time-series samples of each aperture. Raw spectra are then estimated from this time-series using alternate samples, to mimic interleaving. Denote the received voltages at the left aperture TR_1 as e_1 and the right aperture TR_2 as e_2. Since the time series e_2 lags e_1 by one PRT due to this interleaving, a phase compensation is applied to correct for the time offset and is given by

$$e_2(t + t_0) \Longleftrightarrow e^{2\pi f t_0} \quad (7)$$

where, $t_0 = PRT$ and $\Longleftrightarrow$ denotes a Fourier pair. Note that this is mathematically equivalent to interpolating between samples of e_2 in the time domain. Nonetheless, we transform to the time-domain in this work only after applying this phase-compensation in the frequency-domain.

TABLE 1. Nominal simulation parameters.

Parameter	Value
Radar center frequency	9.6 GHz
Pulse repetition frequency	0.5 kHz
Phased-array element spacing	1.6 cm
Number of available elements	64
3-dB beamwidth	3°
Spaced antenna separation	8 cm
Dwell Time	2 s
Range to resolution volume	10 km
Number of scatterers	300
SA baseline wind speed	10 m/s
Cross-baseline wind speed	0 m/s
Radial (Doppler) Velocity	10 m/s
RMS Velocity Turbulence	0 m/s
Signal-to-Noise Ratio	10 dB

3. Validation

In this section, results obtained with the simulator in the absence of velocity turbulence are validated with theoretical predictions. Fig. 3a-b shows the magnitude of the Doppler spectrum and phase of the cross-spectrum respectively for the indicated SNR across the receive array after this phase compensation is applied. As expected, the DFT coefficients in the doppler-spectrum are *spiky* as they are nearly exponentially distributed to begin with. The statistics of these DFT coefficient estimates improve with smoothing or accumulation of periodograms. In this work, we only consider smoothing the periodograms and make no distinction between the duration of the FFT and dwell time. Fig. 3b shows the cross-spectral phase corresponding to Fig. 3a. Notice the linear increase of the cross-spectral phase in the corresponding signal containing part in Fig. 3a. The cross-spectral phase is uniformly distributed from $-\pi$ to π otherwise.

Fig. 4 compares estimated auto- and cross-correlation functions with and without interleaving processing for the indicated SNR at the receive aperture. Note the spike in the cross-correlation function at zero-lag due to thermal noise when the time offset due to interleaving is absent. For interleaving processing, this spike is absent because the cross-correlation coefficient at zero-lag has been estimated by interpolating between lags $+-1$. By virtue of having largely overlapping beams, such spikes at zero-lag have been reported in spaced antenna systems with no overlapping elements. This is because of the relative contribution of the antenna noise temperature to system

noise. For example, Zhang et al. (2004) report that the cross-correlation sample at zero-lag is omitted for processing with the MAPR. The net effect of all this is that active

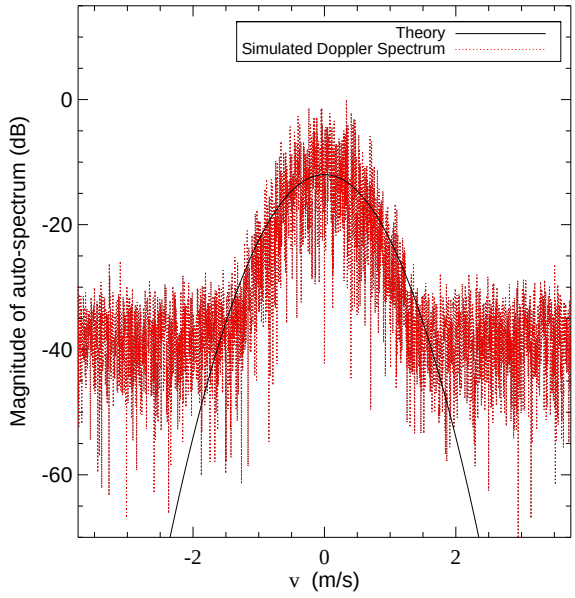

(a)

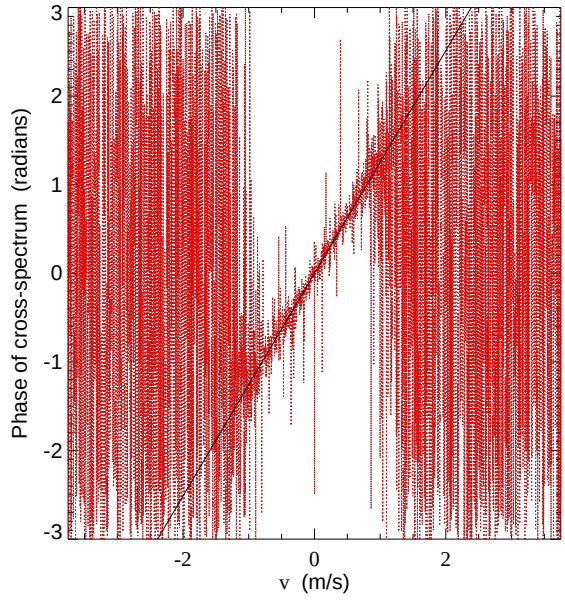

(b)

FIG. 3. a : Magnitude of Doppler spectrum estimates from simulated received Voltages for the indicated SNR at the receive aperture. Fig. b : Cross-spectral phase corresponding to Fig. 3a. The simulation parameters for Fig. 3a-b are indicated in Table b.

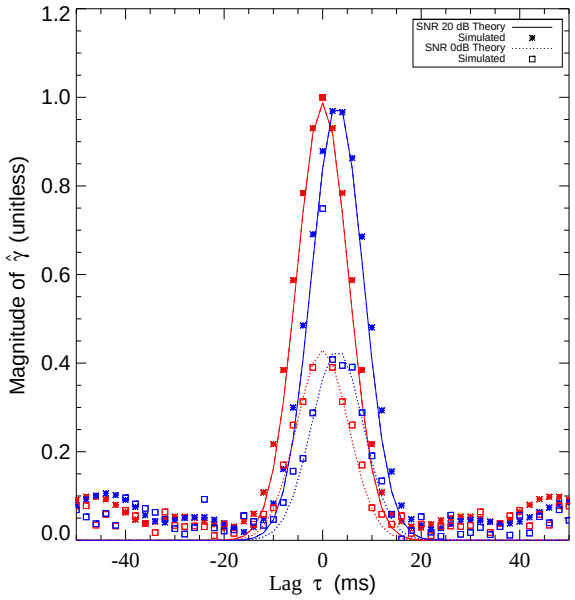

(a)

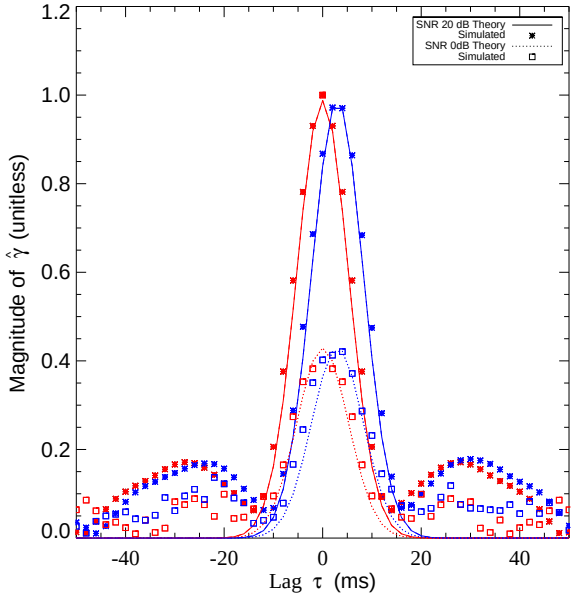

(b)

FIG. 4. Estimated Correlation Coefficients from simulated received Voltages at the phased-array antenna elements in the absence of velocity turbulence for simulation parameters indicated in Table b. Fig. a - No offset. Fig. b - Processing with time offset of 1 PRT. Lines indicate Eqn. (1) multiplied by $\gamma_{SNR} = \frac{1}{1+\frac{1}{SNR}}$ and the scatter points correlation coefficient estimates. Auto-correlation functions are centered at zero-lag and Cross-correlation functions are centered at non-zero lags. Note the spike at zero-lag in the cross-correlation function that scales with SNR for no offset alone.

phased-array implementations lose little information due to interleaving. By virtue of having more overlapping elements, these SA implementations possibly offer the advantage of lesser errors due to RF beamforming as compared to monopulse implementations (which Zhang and Doviak (2007) shows to be equivalent to receiving with L/R aperture halves).

4. Summary and Future Work

This paper describes a spaced-antenna implentation using an X-band active phased-array antenna system in development at the University of Massachusetts. Flexible control of the aperture upon transmit and receive enables alternating portions of the array to be used for alternate pulse, thereby synthesizing interleaved spaced apertures. A monte-carlo based weather radar simulator was developed to simulate backscattered receive voltages at the antenna elements. These simulated voltages at the antenna elements can be combined to mimic the described spaced-antenna system. The results obtained were validated with theoretical predictions for the auto- and cross-spectra and the correlation function expectations. The simulator developed herein can be used to arrive at designs for subsequent implementation and as a tool to better interpret observations from the phased-array spaced-antenna system.

Acknowledgment

Acknowledgment

Acknowledgment

This work was supported by NSF Grant AGS-0937768 to the University of Massachusetts and by the Engineering Research Centers Program of the NSF under Award Number 0313747 to the Center for Collaborative Adaptive Sensing of the Atmosphere (CASA). Any opinions, findings, conclusions, or recommendations expressed in this material are those of the authors and do not necessarily reflect those of the NSF.

REFERENCES

Briggs, B. H., 1984: The analysis of spaced sensor records by correlation techniques. *Middle Atmosphere Program: Handbook for MAP*, R. A. Vincent, Ed., Univ. of Ill., Urbana, Vol. 13, 166–186.

Briggs, B. H., G. J. Phillips, and D. H. Shinn, 1950: The analysis of observations on spaced receivers of the fading of radio signals. *Proc. Phys. Soc. London, B*, **63**, 106–121.

Cheong, B. and R. D. Palmer, 2008: A time-series weather radar simulator based on high-resolution atmpospheric models. *J. Atmos. Oceanic. Tech.*, **25**, 230–243.

Cohn, S. A., W. O. J. Brown, C. L. Martin, M. E. Susedik, G. MacLean, and D. B. Parsons, 2001: Clear air boundary layer spaced antenna wind measurement with the multiple antenna profiler (MAPR). *Ann. Geophys.*, **19 (8)**, 845–854.

Cohn, S. A., C. L. Holloway, S. P. Oncley, R. J. Doviak, and R. J. Lataitis, 1997: Validation of a UHF spaced antenna wind profiler for high-resolution boundary layer observations. *Radio Sci.*, **32**, 1279–1296.

Doviak, R. J., R. J. Lataitis, and C. L. Holloway, 1996: Cross correlations and cross spectra for spaced antenna wind profilers part i: Theoretical analysis. *Radio Sci.*, **31**, 157–180.

Doviak, R. J. and D. S. Zrnić, 1993: *Doppler Radar and Weather Observations, 2nd ed.* Academic Press.

Hardwick, K., S. Frasier, A. Pazmany, H. Bluestein, and M. French, 2005: Spaced antenna measurements of cross beam velocity in severe storms. *32nd Conference on Radar Meteorology*, AMS, Albuquerque, NM, P4R.11.

Holdsworth, D. and I. M. Reid, 1995: A simple model of atmospheric radar backscatter: Description and application to the full correlation analysis of spaced-antenna data. *Radio Sci.*, **30**, 1263–1280.

Holloway, C. L., R. J. Doviak, S. A. Cohn, R. J. Lataitis, and J. S. V. Baelen, 1997: Cross correlations and cross spectra for spaced antenna wind profilers part ii: Algorithms to estimate wind and turbulence. *Radio Sci.*, **32**, RS3017, doi:10.1029/2003RS003 022.

Larsen, M. F. and J. Röttger, 1989: The spaced antenna technique for radar wind profiling. *J. Atmos. Oceanic. Tech.*, **6**, 920–938.

Pazmany, A., H. B. Bluestein, M. M. French, and S. Frasier, 2004: Observations of the two-dimensional wind field in severe convective storms using a mobile X-band Doppler radar with a spaced antenna. *22nd Conference on Severe Local Storms*, AMS, Hyannis, MA, P7.3.

Salazar, J. L., R. Medina, E. J. Knapp, and D. J. McLaughlin, 2008: Phase-tilt array antenna design for dense distributed radar networks for weather sensing. *Int'l. Geosci. & Remote Sensing Symposium*, IEEE, Boston, MA, V–318 – V–321.

Zhang, G., R. Doviak, J. Vivekanandan, and T.-Y. Yu, 2003: Angular and range interferometry to measure wind. *Radio Sci.*, **38**, doi:10.1029/2003RS002 927.

Zhang, G. and R. J. Doviak, 2007: Spaced-antenna interferometry to measure crossbeam wind, shear and turbulence: Theory and formulation. *J. Atmos. Oceanic. Tech.*, **24**, 791–805.

Zhang, G., R. J. Doviak, J. Vivekanandan, W. Brown, and S. Cohn, 2004: Performance of correlation estimators for spaced-antenna wind measurement in the presence of noise. *Radio Sci.*, **92**, 967–982.

Zrnic, D., 1975: Simulation of weatherlike doppler spectra and signals. *J. Appl. Meteor.*, **14**, 619–620.